Abstracta

Ano X - N. 06

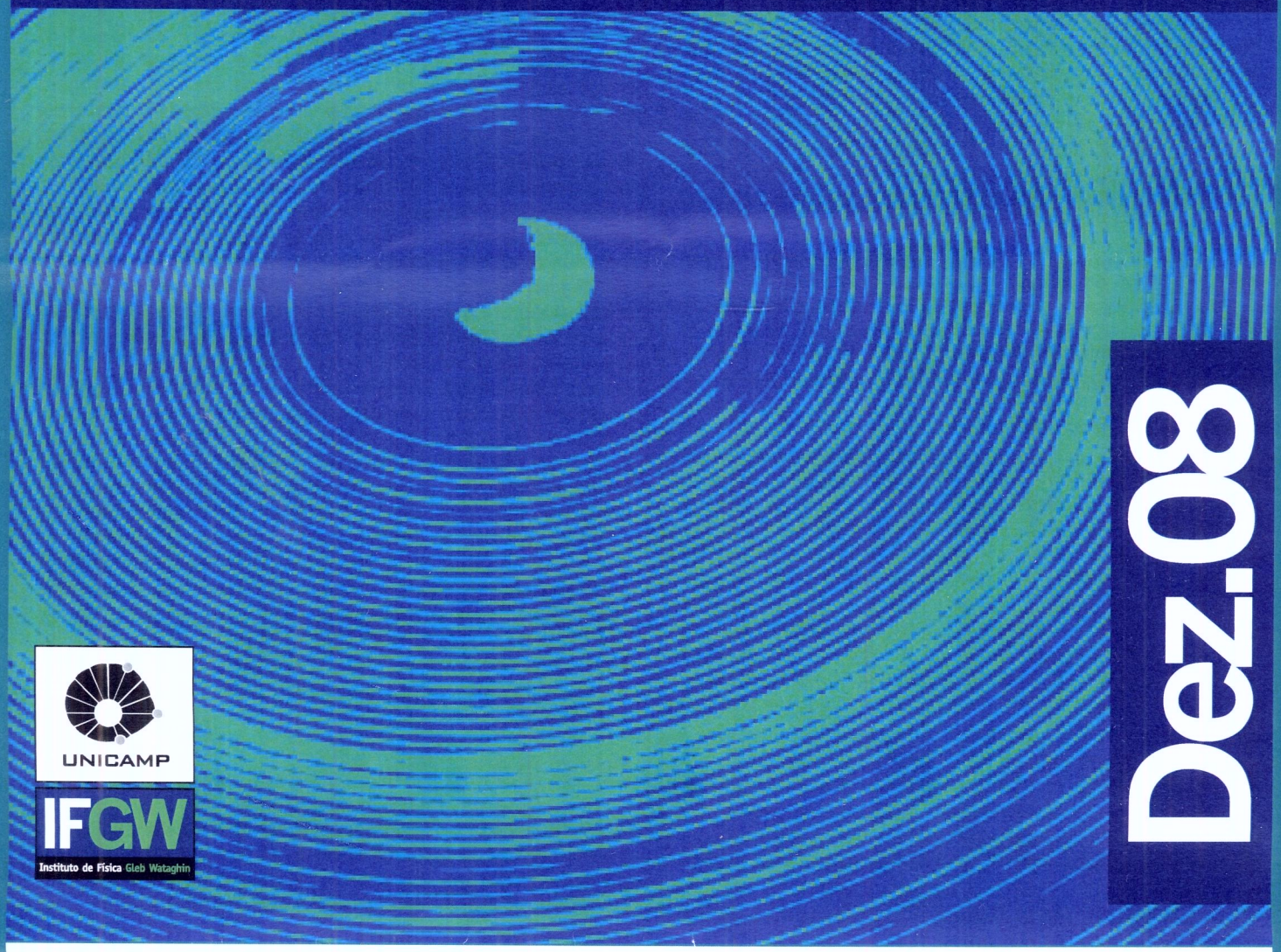

Dez.08

UNICAMP

IFGW

Instituto de Física Gleb Wataghin

Trabalhos Publicados

Novembro 2008 à Dezembro 2008

P 234-08 à P 275-08

Trabalhos Publicados

P234-08 "A comparative study on low-energy elastic electron-NHX (X=1,2,3) collisions"

Brescansin, L. M., Lee, M. T., and Machado, L. E.

In this work, a theoretical study on elastic electron-NHx (x = 1,2,3) collisions in the low-energy range is presented. More specifically, calculated elastic differential, integral, and momentum transfer cross-sections are reported in the (1-30)-eV energy range. An optical potential composed of static, exchange, and correlation-polarization contributions is used to represent the electron-target interaction whereas the iterative Schwinger variational method and the method of continued fractions are used to solve the scattering equations. Comparison of the calculated cross-sections for electron scattering by these targets shows that the results are very similar to each other at higher incident energies. This similarity indicates that the interaction between the scattering electron and the central Nitrogen is dominant. (C) 2008 Wiley Periodicals, Inc

International Journal of Quantum Chemistry **108[13], 2312-2317. 2008.**

P235-08 "Additional levels between Landau bands due to vacancies in graphene: Towards defect engineering"

Pereira, A. L. C. and Schulz, P. A.

We describe the effects of vacancies on the electronic properties of a graphene sheet in the presence of a perpendicular magnetic field: from a single defect to an organized vacancy lattice. An isolated vacancy is the minimal possible inner edge, showing an antidotlike behavior, which results in an extra level between consecutive Landau levels. Two close vacancies may couple to each other, forming a vacancy molecule tuned by the magnetic field. We show that a vacancy lattice introduce an extra band in between Landau levels with localization properties that could lead to extra Hall resistance plateaus

Physical Review B **78[12]. 2008.**

P236-08 "Band edge states of the < n >=0 gap of Fibonacci photonic lattices"

Bruno-Alfonso, A., Reyes-Gomez, E., Cavalcanti, S. B., and Oliveira, L. E.

The stationary and normally incident electromagnetic modes in Fibonacci lattices with generating layers of positive and negative indices of refraction are calculated by a transfer-matrix technique. It is shown that the condition for constructive interference of reflected waves is fulfilled when the ratio of optical paths in positive and negative media are given by the golden ratio. Furthermore, in the long-wavelength limit, it is demonstrated that the edges of the < n > = 0 gap are the frequencies satisfying the conditions <epsilon > = 0 and <mu > = 0

Physical Review A **78[3]. 2008.**

P237-08 "Characterization of photorefractive undoped and doped sillenite crystals using holographic and photoconductivity techniques"

Frejlich, J., Montenegro, R., dos Santos, T. O., and Carvalho, J. F.

We use photoconductivity and holographic techniques to characterize some material and transport properties in undoped and doped photorefractive sillenite crystals, with particular emphasis on photorefractive Bi12TiO20. We show how different dopants are able to modify the performance of the undoped crystals and suggest some possible mechanisms to explain some of their properties

Journal of Optics A-Pure and Applied Optics **10[10]. 2008.**

P238-08 "Comparative study of electron and positron scattering by H-2: The role of the (2)Sigma(+)(g) Feshbach resonance"

Oliveira, E. M., Lima, M. A. P., and Varella, M. T. D. N.

We report two-channel calculations for e(+/-)-H-2 scattering (X-1 Sigma(+)(g)-> X-1 Sigma(+)(g),B-3 Sigma(+)(u) for electrons and X-1 Sigma(+)(g)-> X-1 Sigma(+)(g),B-1 Sigma(+)(u) for positrons). We provide independent estimates of the electron (2)Sigma(+)(g) Feshbach resonance (though for a limited range of interatomic distances) in good agreement with benchmark calculations [D. T. Stibbe and J. Tennyson, J. Phys. B 31, 815 (1998)]. Resonance enhanced vibrational excitation cross sections were obtained with a time-dependent local complex potential approach and compare favorably with recent calculations [R. Celiberto , Phys. Rev. A 77, 012714 (2008)] and experimental data. The time resolution also provides good physical insight into the transient dynamics. In a previous work, we predicted the existence of a positron-hydrogen (2)Sigma(+)(g) Feshbach resonance based on a fixed-nuclei scattering calculation (equilibrium geometry) that was not observed experimentally [J. P. Sullivan , J. Phys. B 34, L467 (2001)]. We further investigate the resonance potential in this study and our results indicate that the (2)Sigma(+)(g) potential crosses the B-1 Sigma(+)(u) state just above the equilibrium interatomic distance of the ground state, giving rise to a short-lived transient. Though the positronium formation channel could also play a role, the state crossing sheds light on the controversy between theory and experiment

Physical Review A **78[4]. 2008.**

P239-08 "Computer simulations of copper and gold nanowires and single-wall nanowires"

Amorim, E. P. M., da Silva, A. J. R., and da Silva, E. Z.

Copper and gold nanowires under tension evolve to form linear atomic chains (LACs), and the study and understanding of this evolution is an important subject for the development of nanocontacts. Here we study the differences and similarities between copper and gold nanowires (NWs) under stress along the [111] crystallographic direction until their rupture using tight-binding molecular dynamics. In both metals, the first significant rearrangement occurs due to one inside atom that goes to the NW' surface. In an attempt to better understand this effect, for both metals we also consider hollow NW's where the inside atoms were excluded after the initial relaxation to create single-wall NW's (SWNWs). The dynamical evolution of these SWNWs provides insight on the formation of the constriction that evolves to form LACs. Studying the calculated forces supported by the NW's we show that SWNWs can sustain larger forces before the first major rearrangement in the copper and gold when compared to the original NW's

Journal of Physical Chemistry C **112[39], 15241-15246. 2008.**

P240-08 "Conserved Central Domains Control the Quaternary Structure of Type I and Type II Hsp40 Molecular Chaperones"

Ramos, C. H. I., Oliveira, C. L. P., Fan, C. Y., Torriani, I. L., and Cyr, D. M.

Heat shock protein (Hsp)40s play an essential role in protein metabolism by regulating the polypeptide binding and release cycle of Hsp70. The Hsp4o family is large, and specialized family members direct Hsp70 to perform highly specific tasks. Type I and Type II Hsp40s, such as yeast Ydj1 and Sis1, are homodimers that dictate functions of cytosolic Hsp70, but how they do so is unclear. Type 1 Hsp40s contain a conserved, centrally located cysteine-rich domain that is replaced by a glycine- and methionine-rich region in Type 11 Hsp40s, but the mechanism by which these unique domains influence Hsp40 structure and function is unknown. This is the case because high-resolution structures of full-length forms of these Hsp40s have not been solved. To fill this void, we built low-resolution models of the quaternary structure of Ydj1 and Sis1 with information obtained from biophysical measurements of protein shape, small-angle X-ray scattering, and ab initio protein modeling. Low-resolution models were also calculated for the chimeric Hsp40s YSY and SYS, in which the central domains of Ydj1. and Sis1 were exchanged. Similar to their human homologs, Ydj1 and Sis1 each has a unique shape with major structural differences apparently being the orientation of the J domains relative to the long axis of the dimers. Central domain swapping in YSY and SYS correlates with the switched ability of YSY and SYS to perform unique functions of Sis1 and Ydj1, respectively. Models for the mechanism by which the conserved cysteine-rich domain and glycine- and methionine-rich region confer structural and functional specificity to Type I and Type 11 Hsp40s are discussed. (C) 2008 Elsevier Ltd. All rights reserved

Journal of Molecular Biology **383[1], 155-166. 2008.**

P241-08 "Effective anisotropy field variation of magnetite nanoparticles with size reduction"

Vargas, J. M., Lima, E., Zysler, R. D., Duque, J. G. S., De Biasi, E., and Knobel, M.

Size effect on the internal magnetic structure has been investigated on weakly interacting magnetite (Fe3O4) nanoparticles by ferromagnetic resonance experiments at 9.5 GHz as a function of temperature (4-300 K). A set of three samples with mean particle size of 2.5 nm, 5.0 nm and 13.0 nm, respectively, were prepared by chemical route with narrow size distribution (sigma < 0.27). To minimize the dipolar interaction, the particles were dispersed in a liquid and a solid polymer matrix at similar to 0.6% in mass. By freezing the liquid suspension with an applied external field, a textured was obtained. Thus, both random and textured suspensions were studied and compared. The ferromagnetic resonance experiments in zero-field-cooled and field-cooled conditions were carried out to study the size effect on the effective anisotropy field. The dc magnetization measurements clearly show that the internal magnetic structure was strongly affected by the particle size

European Physical Journal B **64[2], 211-218. 20**

P242-08 "Effect of a highly concentrated lipopeptide extract of Bacillus subtilis on fungal and bacterial cells"

ETCHEGARAY, A., BUENO, C. D., TESCHKE, O. et all

Lipopeptides produced by Bacillus subtilis are known for their high antifungal activity. The aim of this paper is to show that at high concentration they can damage the surface ultra-structure of bacterial cells. A lipopeptide extract containing iturin and surfactin (5 mg mL-1) was prepared after isolation from B. subtilis (strain OG) by solid phase extraction. Analysis by atomic force microscope (AFM) showed that upon evaporation, lipopeptides form large aggregates (0.1-0.2 mu m2) on the substrates silicon and mica. When the same solution is incubated with fungi and bacteria and the system is allowed to evaporate, dramatic changes are observed on the cells. AFM micrographs show disintegration of the hyphae of Phomopsis phaseoli and the cell walls of Xanthomonas campestris and X. axonopodis. Collapses to fungal and bacterial cells may be a result of formation of pores triggered by micelles and lamellar structures, which are formed above the critical micelar concentration of lipopeptides. As observed for P. phaseoli, the process involves binding, solubilization, and formation of novel structures in which cell wall components are solubilized within lipopeptide vesicles. This is the first report presenting evidences that vesicles of uncharged and negatively charged lipopeptides can alter the morphology of gram-negative bacteria

Archives of Microbiology **190[6], 611-622. 2008.**

P243-08 "Effects of hydrostatic pressure on the electron g(parallel to) factor and g-factor anisotropy in GaAs-(Ga, Al) As quantum wells under magnetic fields"

Porras-Montenegro, N., Duque, C. A., Reyes-Gomez, E.,and Oliveira, L. E.

The hydrostatic-pressure effects on the electron-effective Lande g(parallel to) factor and g-factor anisotropy in semiconductor GaAs-Ga1-xAlxAs quantum wells under magnetic fields are studied. The g(parallel to) factor is computed by considering the non-parabolicity and anisotropy of the conduction band through the Ogg-McCombe effective Hamiltonian, and numerical results are displayed as functions of the applied hydrostatic pressure, magnetic fields, and quantum-well widths. Good agreement between theoretical results and experimental measurements in GaAs-(Ga, Al) As quantum wells for the electron g factor and g-factor anisotropy at low values of the applied magnetic field and in the absence of hydrostatic pressure is obtained. Present results open up new possibilities for manipulating the electron-effective g factor in semiconductor heterostructures

Journal of Physics-Condensed Matter **20[46]. 2008.**

P244-08 "Estimation of the thickness and the optical parameters of several stacked thin films using optimization"
Andrade, R., Birgin, E. G., Chambouleyron, I., Martinez, J. M., and Ventura, S. D.

The reverse engineering problem addressed in the present research consists of estimating the thicknesses and the optical constants of two thin films deposited on a transparent substrate using only transmittance data through the whole stack. No functional dispersion relation assumptions are made on the complex refractive index. Instead, minimal physical constraints are employed, as in previous works of some of the authors where only one film was considered in the retrieval algorithm. To our knowledge this is the first report on the retrieval of the optical constants and the thickness of multiple film structures using only transmittance data that does not make use of dispersion relations. The same methodology may be used if the available data correspond to normal reflectance. The software used in this work is freely available through the PUMA Project web page (http://www.ime.usp.br/similar to egbirgin/puma/). (C) 2008 Optical Society of America

Applied Optics **47[28], 5208-5220. 2008.**

P245-08 "Evidence for the monoclinic-tetragonal phase coexistence in Pb(Zr0.53Ti0.47)O-3 thin films"

Araujo, E. B., Lima, E. C., Guerra, J. D. S., dos Santos, A. O., Cardoso, L. P., and Kleinke, M. U.

The structure and ferroelectric properties of PbZr0.53Ti0.47O3 thin films were investigated in detail by using the x-ray diffraction technique. The surface morphology of the film was studied by using the atomic force microscopy technique, showing a film with a dense morphology and a smooth surface. Based on recent results reported by Pandey et al (2008 Acta Crystallogr. A 64 192), Rietveld refinements of the structure were conducted considering different models proposed in the literature. Results suggested the monoclinic and tetragonal (M + T) phase coexistence, with P4mm and Cm space groups, respectively. The monoclinic phase (68 mol%) is dominant over the tetragonal phase (32 mol%) for this PZT film composition

Journal of Physics-Condensed Matter 20[41]. 2008.

P246-08 "Grain Size Effect on the Structural Parameters of the Stress Induced epsilon(hcp) - Martensite in Iron-Based Shape Memory Alloy"

Nascimento, F. C., Mei, P. R., Cardoso, L. P., and Otubo, J.

The aim of this work was to study the effect of austenitic grain size (GS) reduction on the structural parameters of the epsilon(hcp)-martensite in stainless shape memory alloy (SMA). Rietveld refinement data showed an expansion in c-axis and a reduction in a and b-axis with thermo-mechanical cycles for all samples analyzed. Samples with 75 <= GS (mu m) = 129 were analyzed. It was also observed an increase of the unit cell volume in this phase with GS reduction. The smallest grain size sample (GS = 75 mu m) presented a c/a ratio of 1.649, and approximately 90% of total shape memory recovery

Materials Research-Ibero-American Journal of Materials 11[1], 63-67. 2008.

P247-08 "Hadronic resonance production in d plus Au collisions at <radical><radicand>s(NN)</radicand></radical>=200 GeV measured at the BNL Relativistic Heavy Ion Collider"

Abelev, B. I., Aggarwal, M. M., Ahammed, Z., Anderson, B. D.,

We present the first measurements of the rho(770)(0),K-*(892),Delta(1232)(++),Sigma(1385), and Lambda(1520) resonances in d+Au collisions at <radical><radicand>s(NN)</radicand></radical>=200 GeV, reconstructed via their hadronic decay channels using the STAR detector (the solenoidal tracker at the BNL Relativistic Heavy Ion Collider). The masses and widths of these resonances are studied as a function of transverse momentum p(T). We observe that the resonance spectra follow a generalized scaling law with the transverse mass m(T). The <p(T)> of resonances in minimum bias collisions are compared with the <p(T)> of pi,K, and <overline>p</overline>. The rho(0)/pi(-),K-*/K-,Delta(++)/p,Sigma(1385)/Lambda, and Lambda(1520)/Lambda ratios in d+Au collisions are compared with the measurements in minimum bias p+p interactions, where we observe that both measurements are comparable. The nuclear modification factors (R-dAu) of the rho(0),K-*, and Sigma(*) scale with the number of binary collisions (N-bin) for p(T)> 1.2 GeV/c

Physical Review C 78[4]. 2008.

P248-08 "Helical [110] gold nanowires make longer linear atomic chains"

Amorim, E. P. M. and da Silva, E. Z.

Quantum mechanical molecular dynamics shows that gold nanowires formed along the [110] direction reconstruct upon stress to form helical nanowires. The mechanism for this formation is discussed. These helical nanowires evolve on stretching to form linear atomic chains. Because helical nanowires do not form symmetrical tips, a requirement to stop the growth of atomic chains, these nanowires produce longer atomic chains than other nanowires. These results are obtained resorting to the use of tight-binding molecular dynamics and ab initio electronic structure calculations

Physical Review Letters 101[12]. 2008.

P249-08 "Heterostructure interface roughness characterization by chemical mapping: Application to InGaP/GaAs quantum wells"

Tizei, L. H. G., Bettini, J., Carvalho, M. M. G., and Ugarte, D.

Interface quality is an important factor for the functionality of semiconductor modern devices. Routinely, these characteristics are probed qualitatively by photoluminescence. However, quantitative microscopic structural information to corroborate models is not commonly available. Among different techniques, atomic resolution transmission electron microscopy images represent the basic experimental method to analyze the quality of buried interfaces. In this work we describe the analysis of chemical changes determined from the quantitative comparison of intensity distribution across an interface in high resolution transmission electronic microscopy (HRTEM) images. We have shown that a careful analysis of HRTEM images contrast can provide extremely useful quantitative information on interface roughness. We have characterized four different samples of InGaP/GaAs quantum wells grown with different interfacial schemes. Limits in the quantification from different sources, such as sample preparation, sampling, and statistics, have been thoroughly analyzed. (C) 2008 American Institute of Physics. [DOI: 10.1063/1.2990064]

Journal of Applied Physics 104[7]. 2008.

P250-08 "Human regulatory protein Ki-1/57 has characteristics of an intrinsically unstructured protein"

Bressan, G. C., Silva, J. C., Borges, J. C., dos Passos, D. O., Ramos, C. H. I., Torriani, I. L., and Kobarg, J.

The human protein Ki-1/57 was first identified through the cross reactivity of the anti-CD30 monoclonal antibody Ki-1; in Hodgkin lymphoma cells. The expression of Ki-1/57 in diverse cancer cells and its phosphorylation in peripheral blood leukocytes after mitogenic activation suggested its possible role in cell signaling. Ki-1/57 interacts with several other regulatory proteins involved in cellular signaling, transcriptional regulation and RNA metabolism, suggesting it may have pleiotropic functions. In a previous spectroscopic analysis, we observed a low content of secondary structure for Ki-1/57 constructs. Here, Circular dichroism experiments, in vitro RNA binding analysis, and limited proteolysis assays of recombinant Ki-1/57(122-413) and proteolysis assays of endogenous full length protein from human HEK293 cells suggested that Ki-1/57 has characteristics of an intrinsically unstructured protein. Small-angle X-ray scattering (SAXS) experiments were performed with the C-terminal fragment

Ki-1/57(122-413). These results indicated an elongated shape and a partially unstructured conformation of the molecule in solution, confirming the characteristics of an intrinsically unstructured protein. Experimental curves together with ab initio modeling approaches revealed an extended and flexible molecule in solution. An elongated shape was also observed by analytical gel filtration. Furthermore, sedimentation velocity analysis suggested that Ki-1/57 is a highly asymmetric protein. These findings may explain the functional plasticity of Ki-1/57, as suggested by the wide array of proteins with which it is capable of interacting in yeast two-hybrid interaction assays

Journal of Proteome Research 7[10], 4465-4474. 2008.

P251-08 "Influence of the temperature on the structure of an amorphous Ni46Ti54 alloy produced by mechanical alloying"

Gasperini, A. A. M., Machado, K. D., Buchner, S., de Lima, J. C., and Grandi, T. A.

The evolution of the local atomic order of an amorphous Ni46Ti54 alloy produced by mechanical alloying as a function of temperature was studied by synchrotron X-ray diffraction (XRD) and differential scanning calorimetry (DSC) techniques. XRD measurements at several temperatures (25 degrees C, 350 degrees C, 412 degrees C, 430 degrees C, 450 degrees C and 515 degrees C) were performed and analyzed using the reverse Monte Carlo (RMC) simulations method or the Rietveld refinement procedure. The experimental total structure factor for samples at 25 degrees C and 350 degrees C, which are amorphous in nature, were simulated by using the RMC method, and the local structures of the alloy at both temperatures were determined, indicating a decrease in its density as the temperature increases. At 412 degrees C, the XRD pattern shows a partially crystalline sample, indicating that the crystallization process is in progress. At 430 degrees C, 450 degrees C and 515 degrees C, the XRD measurements indicate the presence of two crystalline phases, NiTi and NiTi2, whose structural parameters (lattice parameters, coherently diffracting domains (CDD) sizes, microstrains and relative amount of phases) were determined using the Rietveld refinement procedure. DSC measurements at different heating rates furnished the crystallization temperature, enthalpy and activation energy of the crystallization process, and these values are similar to those found in other amorphous alloys of the Ni-Ti system. They also showed the existence of a second exothermic process, which was related to diffusive processes in the crystalline phases, which could be associated with the changes in the CDD sizes happening from 450 degrees C to 515 degrees C

European Physical Journal B 64[2], 201-209. 2008.

P252-08 "Isothermal variation of the entropy (Delta S-T) for the compound Gd5Ge4 under hydrostatic pressure"

Carvalho, A. M. G., Coelho, A. A., Gama, S., von Ranke, P. J., and Alves, C. S.

In the present work, the isothermal variation of the entropy (Delta S-T) for the compound Gd5Ge4 was studied at different applied hydrostatic pressures (from 0 up to 0.58 GPa). In all pressure ranges, we observe the giant magnetocaloric effect. The AST data for the compound Gd5Ge4 at zero applied pressure present two peaks: the lowest temperature peak is due to irreversible processes and the highest temperature peak is due to magneto structural transitions. Increasing the pressure, the lowest temperature peak displaces to lower temperatures and disappears. The magnitude of the other peak has a nonlinear behavior with pressure. Different protocols were used to obtain Delta S-T at zero applied pressure and the results indicate that Delta S-T strongly depends on the initial and final states of Gd5Ge4 compound. We also present a T-P magnetic phase diagram built from the available magnetic data. (C) 2008 American Institute of Physics. [DOI: 10.1063/1.2980040]

Journal of Applied Physics 104[6]. 2008.

P253-08 "Magnetic resonant x-ray diffraction study of europium telluride"

Diaz, B., Granado, E., Abramof, E., Rappl, P. H. O., Chitta, V. A., and Henriques, A. B.

Here we use magnetic resonant x-ray diffraction to study the magnetic order in a 1.5 mu m EuTe film grown on (111) BaF2 by molecular-beam epitaxy. At Eu L-II and L-III absorption edges, a resonant enhancement of more than two orders was observed for the sigma ->pi(') diffracted intensity at half-order reciprocal-lattice points, consistent with the magnetic character of the scattering. We studied the evolution of the (1/21/21/2) magnetic reflection with temperature. When heating toward the Neel temperature (T-N), the integrated intensity decreased monotonously and showed no hysteresis upon cooling again, indicating a second-order phase transition. A power-law fit to the magnetization versus temperature curve yielded T-N=9.99(1) K and a critical exponent beta=0.36(1), which agrees with the renormalization theory results for three-dimensional Heisenberg magnets. The fits to the sublattice magnetization dependence with temperature, disregarding and considering fourth-order exchange interactions, evidenced the importance of the latter for a correct description of magnetism in EuTe. A value of 0.009 was found for the (2j(1)+j(2))/J(2) ratio between the Heisenberg J(2) and fourth-order j(1,2) exchange constants. The magnetization curve exhibited a round-shaped region just near T-N accompanied by an increase in the magnetic peak width, which was attributed to critical scattering above T-N. The comparison of the intensity ratio between the (1/21/21/2) and the (1/21/21/2) magnetic reflections proved that the Eu2+ spins align within the (111) planes, and the azimuthal dependence of the (1/21/21/2) magnetic peak is consistent with the model of equally populated S domains

Physical Review B 78[13]. 2008.

P254-08 "Measurement of neutrino oscillations with the MINOS detectors in the NuMI beam"

Adamson, P., Andreopoulos, C., Arms, K. E., Armstrong, R., Escobar, C. O.

This Letter reports new results from the MINOS experiment based on a two-year exposure to muon neutrinos from the Fermilab NuMI beam. Our data are consistent with quantum-mechanical oscillations of neutrino flavor with mass splitting vertical bar Delta m(2)vertical bar = (2.43 +/- 0.13) x 10(-3) eV(2) (68% C.L.) and mixing angle sin(2)(2 theta) > 0.90 (90% C.L.). Our data disfavor two alternative explanations for the disappearance of neutrinos in flight: namely, neutrino decays into lighter particles and quantum decoherence of neutrinos, at the 3.7 and 5.7 standard-deviation levels, respectively

Physical Review Letters 101[13]. 2008.

P255-08 "Modeling the auxetic transition for carbon nanotube sheets"

Coluci, V. R., Hall, L. J., Kozlov, M. E., Zhang, M., Dantas, S. O., Galvao, D. S., and Baughman, R. H.

A simple model is developed to predict the complex mechanical properties of carbon nanotube sheets (buckypaper) [L. J. Hall et al., Science 320, 504 (2008)]. Fabricated using a similar method to that deployed for making writing paper, these buckypapers can have in-plane Poisson's ratios changed from positive to negative, becoming auxetic, as multiwalled carbon nanotubes are increasingly mixed with single-walled carbon nanotubes. Essential structural features of the buckypapers are incorporated into the model: isotropic in-plane mechanical properties, nanotubes preferentially oriented in the sheet plane, and freedom to undergo stress-induced elongation by both angle and length changes. The expressions derived for the Poisson's ratios enabled quantitative prediction of both observed properties and remarkable new properties obtainable by structural modification

Physical Review B 78[11]. 2008.

P256-08 "Nonlinear interaction between two different photonic bandgaps of a hybrid photonic crystal fiber"

Arismar, C. S., Cordeiro, C. M. B., Biancalana, F., Roberts, P. J., Hernandez-Figueroa, H. E., and Cruz, C. H. B.

Nonlinear interaction between spectral components in two different photonic bandgaps is experimentally demonstrated by launching femtosecond pulses near a zero-dispersion wavelength of a hybrid photonic crystal fiber, which guides by a combination of total internal reflection and bandgap effects. It is demonstrated that the initial pulse becomes spectrally broadened, and narrowband resonant radiation is generated in a different bandgap from the one responsible for guiding at the pump wavelength. The spectral intensity of the resonant radiation peaks at 2.7 dB below that of the broadened pulse in the pump-guiding bandgap. (C) 2008 Optical Society of America

Optics Letters 33[18], 2080-2082. 2008.

P257-08 "On the elastic constants of amorphous carbon nitride"

Champi, A., Ferlauto, A. S., Alvarez, F., Silva, S. R. P., and Marques, F. C.

Elastic and thermomechanical properties of amorphous carbon nitrite thin films as a function of nitrogen concentration are reported. The films were prepared by ion beam assisted deposition with nitrogen concentrations ranging from 0 to 33 at% By using a combination of the thermally induced bending technique and nano-indentation measurements it was possible to calculate independent values for the Young's modulus, the Poisson's ratio, as well as the thermal expansion coefficient of the films. The hardness and elastic recovery are discussed in terms of the Young's modulus and the Poisson's ratio. (C) 2008 Elsevier B.V. All rights reserved

Diamond and Related Materials 17[11], 1850-1852. 2008.

P258-08 "On the properties of the eutectic alloy Al-3(Nb,Cr)+Cr(Al,Nb)"

Souza, S. A., Ferrandini, P. L., Souza, E. A., dos Santos, A. O., and Caram, R.

The eutectic alloy Al-3(Nb,Cr)+Cr(Al,Nb) forms an insitu composite and the Al3Nb presents high specific strength and low oxidation rate that may be improved by the combination with other phases. The purpose of this work is to investigate physical, mechanical and oxidation properties of the eutectic alloy.Therefore, Rietveld analysis was carried out for furnace cooled and water quenched samples and oxidation tests were performed on directional solidified samples. Compressive tests were performed for the eutectic alloy and also for the Nb-74.8% Cr-24.6% Al alloy in the as-cast condition. The alloy presents 12.9% Cr(Al,Nb) at room temperature, retained from the transformation Cr(Al,Nb) to Al(Nb)Cr-2. The combination of Al3Nb with Cr(Al,Nb) and Al(Nb)Cr, considerably improves mechanical behaviour, leading the yield strength to 1525 MPa at 800 degrees C and 925 MPa at 900 degrees C. The oxidation tests showed the formation of several oxides at all temperatures studied and that from 900 degrees C on alfa Al2O3 is formed both in air and O-2 except under O-2 at 1000 degrees C. It is believed that the Cr(Al,Nb) phase acts as an Al reservoir for the formation of the various Al2O3 scales. (C) 2007 Elsevier B. V. All rights reserved

Journal of Alloys and Compounds 464[1-2], 162-167. 2008.

P259-08 "One-dimensional Kondo lattice model at quarter filling"

Xavier, J. C. and Miranda, E.

We revisit the problem of the quarter-filled one-dimensional Kondo lattice model, for which the existence of a dimerized phase and a nonzero charge gap had been reported by Xavier [Phys. Rev. Lett. 90, 247204 (2003)]. Recently, some objections were raised claiming that the system is neither dimerized nor has a charge gap. In the interest of clarifying this important issue, we show that these objections are based on results obtained under conditions in which the dimer order is artificially suppressed. We use the incontrovertible dimerized phase of the Majumdar-Ghosh point of the J(1)-J(2) Heisenberg model as a paradigm with which to illustrate this artificial suppression. Finally, by means of extremely accurate density-matrix renormalization-group calculations, we show that the charge gap is indeed nonzero in the dimerized phase

Physical Review B 78[14]. 2008.

P260-08 "Optical excitation and characterization of gigahertz acoustic resonances in optical fiber tapers"

Kang, M. S., Brenn, A., Wiederhecker, G. S., and Russell, P. S. J.

Transverse acoustic resonances at gigahertz frequencies are excited by electrostriction in the few-micrometer-thick waists of low-loss optical fiber tapers of up to 40 cm long. A pump-probe technique is used in which the resonances are excited by a train of optical pulses and probed in a Sagnac interferometer. Strong radially symmetric acoustic resonances are observed and the dependence of their frequencies on taper thickness is investigated. Such easily reconfigurable acousto-optic interactions may have applications in the high-frequency mode locking of fiber lasers. (C) 2008 American Institute of Physics

Applied Physics Letters 93[13]. 2008.

P261-08 "Overspinning a nearly extreme black hole and the weak cosmic censorship conjecture"

Richartz, M. and Saa, A.

We revisit here the recent proposal for overspinning a nearly extreme black hole by means of a quantum tunneling process. We show that electrically neutral massless fermions evade

possible backreaction effects related to superradiance, confirming the view that it would be indeed possible to form a naked singularity due to quantum effects

Physical Review D 78[8]. 2008.

P262-08 "Photorefractive two-wave mixing phase coupling measurement in a self-stabilized recording regime"

Montenegro, R., Freschi, A. A., and Frejlich, J.

The measurement of the phase coupling. between the two-wave mixed transmitted and diffracted beams behind a photorefractive material is directly obtained using a self-stabilized recording technique. These phase coupling data are used to compute the Debye screening length on an undoped Bi12TiO20 crystal. The diffraction efficiency, which is obtained in two different ways from the same self-stabilized experimental run, is similarly processed to compute the Debye length too. The Debye length is also measured for Pb- and Zr-doped Bi12TiO20 crystals, and from this parameter the corresponding effective density of traps is computed and shown to be lower than for the undoped sample

Journal of Optics A-Pure and Applied Optics 10[10]. 2008.

P263-08 "Polaron liquid-gas crossover at the orthorhombic-rhombohedral transition of manganites"

Souza, J. A., Terashita, H., Granado, E., Jardim, R. F., Oliveira, N. F., and Muccillo, R.

High-resolution synchrotron x-ray powder diffraction in La0.7Ca0.3MnO3 shows in detail a first-order structural phase transition from orthorhombic (space-group Pnma) to rhombohedral (space-group R (3) over barc) crystal structures near T-S=710 K. Magnetic susceptibility measurements show that the rhombohedral phase strictly obeys the Curie-Weiss law as opposed to the orthorhombic phase. A concomitant change in the electrical resistivity behavior, consistent with an alteration from nonadiabatic to adiabatic small polaron hopping regimes, was also observed at T-S. The simultaneous change in transport and magnetic properties are identified as a transition from a correlated polaron liquid for T<T-S to an uncorrelated polaron gas for T>T-S, driven by the change in the crystal symmetry

Physical Review B 78[5]. 2008.

P264-08 "Positron scattering from formic acid"

Zecca, A., Chiari, L., Sarkar, A., Lima, M. A. P., Bettega, M. H. F., Nixon, K. L., and Brunger, M. J.

We report on measurements of total cross sections for positron scattering from the fundamental molecule formic acid (HCOOH). In this case, the energy range of our experimental work is 0.3-50.2 eV. Our interpretation of these data was somewhat complicated by the fact that at room temperature, formic acid vapor consists of about 95% monomer and 5% dimer forms, so that the present cross sections represent an average for that ensemble. To assist us in interpreting the data, rigorous Schwinger multichannel level calculations for positron elastic scattering from the formic acid monomer were also undertaken. These calculations, incorporating an accurate model for the target polarization, are found to be in good qualitative agreement with our measured data, particularly when allowance is made for the target beam mixture (monomer versus dimer) in the experiment

Physical Review A 78[4]. 2008.

P265-08 Preservation of scientific memory and greater visibility to the scientific production of Institute of Physics Gleb Wataghin of Unicamp

Sponchiado, R.A., Cartaxo. S.M.C.

This paper seeks to progress to a service already systematized the IFGW Library regarding the management of data related to the scientific production of the institute. The goal is to ensure his memory through scientific recovery of the full text of all the scientific production of IFGW indexed in the period from 1972 to 2007. Moreover, it is intended to catalogue this production in bibliographic catalogue of the university helping to increase the visibility and access to knowledge generated in the institute. We introduce the way in which such items are recovered and the progress of this work, showing the total amount of published, recovered and linked articles. We discusses regarding maintenance of institutional repositories, open archives and the Moviment of Free Access to Information and the new forms of access and transmission of knowledge with in the university. We also discourse about the emergence of a new paradigm of Free Electronic Access and seek awareness through this, the discussion of the university community to that. We conclude that the joining of all scientific production of IFGW, but the university, is of fundamental importance for its self-knowledge and its own development

XV Seminário Nacional de Bibliotecas Universitárias. São Paulo, 2008.

P266-08 "Role of X valley on the dynamics of electron transport through a GaAs/AlAs double-barrier structure"

Galeti, H. V. A., de Carvalho, H. B., Brasil, M. J. S. P., Gobato, Y., Lopez-Richard, V., Marques, G. E., Henini, M., and Hill, G.

The transport of electrons through a GaAs/AlAs double-barrier structure with p-type doped contacts was investigated using time-resolved photoluminescence spectroscopy. Under illumination, the current-voltage characteristics of the device present two additional features attributed, respectively, to resonant Gamma-Gamma and Gamma-X electron tunneling. Optical measurements for biases where these two alternative transport mechanisms have competitive probabilities revealed an unusual carrier dynamics. The quantum well emission is strongly delayed and we observe a remarkable nonlinear effect where the emission intensity decreases at the arrival of a laser pulse. We propose a simple model that adequately describes our results where we assume that the indirect-transition rate depends on the density of electrons accumulated along the structure

Physical Review B 78[16]. 2008.

P267-08 "Self-stabilized recording of fixed gratings at high temperature in LiNbO3:Fe"

von Bassewitz, J. P., de Oliveira, I., and Frejlich, J.

A high quality fixed holographic grating was recorded in a photorefractive LiNbO3:Fe crystal at about 100 degrees C in a homemade temperature-controlled vacuum chamber. The recording was carried out using self-stabilization techniques with lambda = 532 nm beams guided onto the crystal by polarization maintaining fibers. The diffraction efficiency of the fixed grating was eta = 0.44 when measured in the recording setup using the same lambda = 532 nm recording beams. A compatible eta was measured with lambda = 633 nm

in an auxiliary setup, and a 1 mrad angular Bragg selectivity at FWMH was estimated, thus demonstrating the uniformity and good quality of the fixed grating. (C) 2008 Optical Society of America

Applied Optics 47[29], 5315-5320. 2008.

P268-08 "Some electronic properties of saturated and unsaturated cubane oligomers using DFT-based calculations"

Konstantinova, E., Camilo, A., Barone, P. M. V. B., Dantas, S. O., and Galvao, D. S.

Cubanes and cubane-based molecular structures attract considerable interest as structural units which represent a new class of materials with remarkable properties. These structures are potentially useful for a variety of industrial applications and, for this reason, deserve detailed study. One of the options is to use cubane-based structures to synthesize a new class of conducting polymers with small energy band gap. In the present work we use the DFT-based methods to perform geometrical optimization and obtain some electronic properties for cubane, cubatriene, saturated and unsaturated oligomers containing different number of cubane and cubatriene building units. Our results indicate that the energy difference between the lowest unoccupied molecular orbital (LUMO) and the highest occupied molecular orbital (HOMO) manifests a small decrease with the growing units number for saturated or unsaturated oligomers. This energy difference is strongly dependent on the presence of hydrogen atoms and is greater for unsaturated structures. (C) 2008 Elsevier B.V. All rights reserved

Journal of Molecular Structure-Theochem 868[1-3], 37-41. 2008.

P269-08 "Some electronic properties of saturated and unsaturated cubane oligomers using DFT-based calculations"

Konstantinova, E., Camilo, A., Barone, P. M. V. B., Dantas, S. O., and Galvao, D. S.

Cubanes and cubane-based molecular structures attract considerable interest as structural units which represent a new class of materials with remarkable properties. These structures are potentially useful for a variety of industrial applications and, for this reason, deserve detailed study. One of the options is to use cubane-based structures to synthesize a new class of conducting polymers with small energy band gap. In the present work we use the DFT-based methods to perform geometrical optimization and obtain some electronic properties for cubane, cubatriene, saturated and unsaturated oligomers containing different number of cubane and cubatriene building units. Our results indicate that the energy difference between the lowest unoccupied molecular orbital (LUMO) and the highest occupied molecular orbital (HOMO) manifests a small decrease with the growing units number for saturated or unsaturated oligomers. This energy difference is strongly dependent on the presence of hydrogen atoms and is greater for unsaturated structures. (C) 2008 Elsevier B.V. All rights reserved

Journal of Molecular Structure-Theochem 868[1-3], 37-41. 2008.

P270-08 "Structural, microstructural and magnetic investigations in high-energy ball milled BiFeO3 and Bi0.95Eu0.05FeO3 powders"

Freitas, V. F., Grande, H. L. C., de Medeiros, S. N., Santos, I. A., Cotica, L. F., and Coelho, A. A.

In this paper, synthesis, structural, microstructural and magnetic properties of high-energy ball milled BiFeO3 and Bi0.95Eu0.05FeO3 powders were thoroughly investigated through X-ray diffraction, scanning electron microscopy, Mossbauer spectroscopy and magnetization measurements. Single-phased compounds were processed by using both mechanosynthesis and post-milling annealing. The set of results did not indicate considerable alterations in the magnetic ordering of the powders, even though their ordering temperature, magnetization and coercivity were highly sensitive to the narrow grain sizes distribution of nanograins and substituting Eu ion. In addition, we have shown that enhanced magnetic properties of BiFe03 could be achieved by a low degree of Eu substitution, yet preserving the structural and microstructural characteristics of the processed powders. (c) 2007 Elsevier B.V. All rights reserved

Journal of Alloys and Compounds 461[1-2], 48-52. 2008.

P271-08 "SU-8 submicrometric sieves recorded by UV interference lithography"

Gutierrez-Rivera, L. E. and Cescato, L.

Sieves are promising devices for filtration, separation of particles and drug delivery control because of their uniform pore size distribution and low flow resistance. SU-8 is a negative photoresist type epoxy that is hydrophobic and biocompatible. Thus, it is a good alternative to fabricate micro devices for biological applications. In this paper we show a novel fabrication technique of self-sustained sieves of an SU-8 photoresist, with pore dimensions in the range of hundreds of nanometers, using a combination of UV interference and conventional optical lithographies. The resulting sieves are SU-8 membranes with submicrometric pore sizes and coefficient of variation of 7%, in areas of 1 cm(2)

Journal of Micromechanics and Microengineering 18[11]. 2008.

P272-08 "Synthesis and magnetic characterization of Pb1-xMnxS nanocrystals in glass matrix"

Silva, R. S., Morais, P. C., Mosiniewicz-Szablewska, E., Cuevas, R. F., Campoy, J. C. P., Pelegrini, F., Qu, F., and Dantas, N. O.

The synthesis of manganese-doped PbS (Pb1-xMnxS) nanocrystal (NC) dots within a borosilicate glass matrix has been investigated by atomic force microscopy, electron paramagnetic resonance and magnetic measurements. The fusion method was employed in the preparation of the magnetic semiconductor NC dots whereas the measurements performed showed changes in the physical properties of the manganese-doped dots as a result of the Mn2+-incorporation into the hosting PbS crystal structure. Nevertheless, the data indicated that only a small fraction of the nominal Mn-doping was incorporated into the PbS NC dot, in both lower (0.5%) and higher (40%) nominal doping ends. For the lower nominal Mn-doping end (0.5%) we found only about 0.05% actually incorporated into the PbS NC dot whereas about 0.45% appeared dispersed throughout the glass template as isolated paramagnetic centres

Journal of Physics D-Applied Physics 41[16]. 2008.

P273-08 "Testing Lorentz Invariance and CPT Conservation with NuMI Neutrinos in the MINOS Near Detector"

Adamson, P., Andreopoulos, C., Arms, K. E., Armstrong, R., Auty, D. J., Ayres, Escobar, C. O.

A search for a sidereal modulation in the MINOS near detector neutrino data was performed. If present, this signature could be a consequence of Lorentz and CPT violation as predicted by the effective field theory called the standard-model extension. No evidence for a sidereal signal in the data set was found, implying that there is no significant change in neutrino propagation that depends on the direction of the neutrino beam in a sun-centered inertial frame. Upper limits on the magnitudes of the Lorentz and CPT violating terms in the standard-model extension lie between 10(-4) and 10(-2) of the maximum expected, assuming a suppression of these signatures by a factor of 10(-17)

Physical Review Letters 101[15]. 2008.

P274-08 "The electronic and optical properties of oligo(trans-1,2-di(2-thienyl)-1,3-butadiene): A theoretical study"

Marcal, N. and Laks, B.

In the present work we investigated the theoretical electronic structure of poly(trans-1,4-di(2-thienyl)-1,3-butadiene) (PTB) and determined the optical properties of its neural and doped oligomers. Geometrical optimizations were at the semiempirical level by using the Austin method 1 (AM1). The band structure of pi electrons regarding to the neutral PTB polymer was obtained by using a tight-binding Hamiltonian. The densities of electronic states (DOS) for neutral and doped copolymers were calculated by using the negative factor counting technique. The spatial charge distribution of the oligomeric chain was also analyzed. The energy of the electronic transitions and their associated oscillator strength values were calculated for the neutral, double, and single charged oligomers to determine the UV-vis absorption spectra. The calculations were performed using the intermediate neglect of differential overlap Hamiltonian in combination with the single configuration-interaction technique in order to include correlation effects. The band gap obtained in the PTB was about 2.101 eV for the optics absorption and 1.73 eV for the DOS. The bipolaron states appear in the gap, about 0.57 eV and 0.48 eV below and above the conduction and valence bands, respectively. When the dopants concentration is increased the DOS showed that the energy gap tends to vanish, which may lead to semiconductor-metal transition. (C) 2008 Wiley Periodicals, Inc

International Journal of Quantum Chemistry 108[13], 2499-2506. 2008.

P275-08 "The speckle photo-electromotive force on a vanadium-doped CdTe crystal"

Santos, T. O., Launay, J. C., Odoulov, S. G., and Frejlich, J.

The photo-electromotive force (photo-emf) generated by a vibrating laser speckle pattern at 1064 nm in the bulk of a photorefractive vanadium-doped CdTe crystal is used to evaluate the sample's response time and the vibration amplitude of the speckle pattern. We measured the first harmonic temporal term of the photocurrent, under different conditions, as a function of the vibration amplitude, vibration frequency, and irradiance, in order to verify some features of the theoretical model for large vibration amplitude speckle photo-emf. The most interesting feature is the presence, for sufficiently fast vibrations, of a maximum in this first harmonic term at a fixed vibration amplitude-to-speckle size ratio whose position should depend only on the dark conductivity to photoconductivity ratio. The presence of such a maximum is confirmed and opens the way for rather simple calibration of the setup in practical applications. We also demonstrate the application of this photo-emf signal to evaluate the material response time of the CdTe: V crystal

Journal of Optics A-Pure and Applied Optics 10[10]. 2008.

Abstracta

Instituto de Física
Diretor: Prof. Dr. Julio Cesar Hadler Neto
Universidade Estadual de Campinas - UNICAMP
Cidade Universitária C.P. 6165
CEP: 13081-970 - Campinas - SP - Brasil
e-mail: secdir@ifi.unicamp.br
Fone: 0XX 19 3521-5300

Publicação

Biblioteca do Instituto de Física Gleb Wataghin
http://webbif.ifi.unicamp.br
Diretora Técnica: Rita Aparecida Sponchiado

Elaboração
Antonela Carvalho Ribeiro
antonela@ifi.unicamp.br

Projeto Gráfico
ÍgneaDesign

Impressão
Gráfica Central - Unicamp